Combustion and Flame 199 (2019) 230–240

Contents lists available at ScienceDirect

Combustion and Flame

journal homepage: www.elsevier.com/locate/combustflame

Effect of H_2O and CO_2 on propane, propene, and isopropanol oxidation at elevated pressures

Oxana N. Fedyaeva*, Denis O. Artamonov, Anatoly A. Vostrikov

Kutateladze Institute of Thermophysics SB RAS, 1, Acad. Lavrentyev Av., Novosibirsk, Russia

ARTICLE INFO

Article history:
Received 12 August 2018
Revised 27 September 2018
Accepted 27 September 2018
Available online 1 November 2018

Keywords:
Propane
Propene
Isopropanol
Self-ignition
Carbon dioxide
Water vapor

ABSTRACT

The article discusses research results on oxidation features of high-density fuel-enriched C_3H_8/O_2, C_3H_6/O_2, and C_3H_7OH/O_2 mixtures ($\rho_{fuel} = 0.22–0.25$ mol/dm^3, $\rho_{O2} = 0.76–0.88$ mol/dm^3) diluted with argon, carbon dioxide, or water vapor (from 59 to 72% mol.) at the uniform heating (1 K/min) of tubular reactor to 640 K. Proceeding from the time dependences of the reaction mixtures temperature, it was revealed that the self-ignition temperature of fuels in the Ar medium increases in the following sequence: $C_3H_6 < C_3H_7OH < C_3H_8$. The self-ignition temperature of propane and propene is almost independent of the diluent nature, while the self-ignition temperature of isopropanol in the diluents medium increases in the following sequence: $Ar < CO_2 < H_2O$. The chain-thermal explosion was observed during the propane oxidation in Ar and H_2O media, as well as during the isopropanol oxidation in Ar and CO_2 media. Using mass spectrometric analysis, it was shown that the oxidation of propane in CO_2 medium is characterized by a low degree of fuel conversion at almost complete consumption of O_2, while the oxidation of propene is characterized by a low degree of fuel conversion and O_2 consumption. Oxidation of fuels in the H_2O medium occurs in several stages and is characterized by almost complete consumption of O_2. In this paper we consider the mechanisms of chemical involvement of CO_2 and H_2O molecules in fuel oxidation.

1. Introduction

Combustion of fossil fuels and organic wastes directly in the heat carrier (supercritical water and carbon dioxide) increases energy efficiency and ecological cleanness of heat and electric energy production [1–5]. It is obvious that in order to develop new technologies based on combustion of different types of fuels in supercritical water and carbon dioxide, it is necessary to identify combustion features of individual compounds in these media. Earlier we have studied the combustion of hydrogen, methane, and isobutane in the nitrogen, carbon dioxide, and water vapor media [6–8]. The aim of the present work is to identify the features of propane, propene, and isopropanol combustion in high-density fuel/O_2/Ar, fuel/O_2/CO_2, and fuel/O_2/H_2O mixtures. The choice of these fuels as the research objects is due to the following. From the results [9,10], it follows that alkenes are ones of the alkanes conversion products in supercritical water. Propene is the simplest hydrocarbon containing single and double carbon-carbon bonds. Isopropanol, according to [11], is one of the products of propene conversion in supercritical water. A comparative analysis of the oxidation results of these fuels will allow revealing the regularities of the conversion of the main classes of aliphatic hydrocarbons in the water and carbon dioxide media.

The interest in the study of the propane and propene combustion is caused primarily by the fact that these substances are components of liquefied petroleum gas. Merchant at al. [12] proposed a detailed kinetic mechanism (DKM) of the initial stages of low-temperature (600–800 K, 0.1 MPa) oxidation of propane. According to [12], the oxidation is initiated by the hydrogen atom abstraction from propane in the reaction

$$C_3H_8 + O_2 \rightarrow C_3H_7 + HO_2. \quad (1)$$

The subsequent interaction of C_3H_7 radicals with oxygen leads to formation of peroxypropyl radicals

$$C_3H_7 + O_2 \rightarrow C_3H_7O_2. \quad (2)$$

Accumulation of $C_3H_7O_2$ radicals and their subsequent decomposition, proceeding through rearrangement into hydroperoxypropyl radicals

$$C_3H_7O_2 \rightarrow C_3H_6OOH \rightarrow C_3H_6O + HO, \quad (3)$$

determine the ignition delay time [12].

* Corresponding author.
E-mail addresses: fedyaeva@itp.nsc.ru, oxana.fedyaeva@mail.ru (O.N. Fedyaeva).

https://doi.org/10.1016/j.combustflame.2018.09.031
0010-2180/

Nomenclature

Roman symbols

C	heat capacity, J/K
DKM	detailed kinetic mechanism
H	enthalpy, J/mol
MIE	minimum ignition energy
NTC	negative temperature coefficient
P	pressure, MPa
q	heating rate, K/min
Q	heat release, J
S	area, K·min
SCWO	supercritical water oxidation
t	time, min
T	temperature, K
x	molar fraction, % mol.

Greek symbols

α	conversion degree, % mol.
Δ	increment
ε	stoichiometric coefficient
λ	thermal conductivity, W/m•K
ν	vibrational frequency, cm^{-1}
ρ	density, mol/dm^3
σ	standard deviation
φ	fuel equivalence ratio

Superscript

*	parameter of self-ignition

Subscript

ad	adiabatic
d	diluent
ev	evaporation
f	fuel
i	component
in	internal thermocouple
j	vibrational level
O	oxygen
out	outer thermocouple
ox	oxidation
R	residue
v	isochoric

Prince and Williams [13] studied the ignition of propane/air mixture (500–1000 K, 0.1 MPa) by numerical methods and proposed the mechanisms of two-stage ignition and the behavior of the negative temperature coefficient (NTC) of the reaction rate. Based on the comparison of numerical and experimental data, the authors [13] concluded that the proposed kinetic model is in good agreement with the results obtained by means of the rapid compression machine, but differs from the results obtained in the autoclave due to the approximate account of the radical loss on its wall. Norman et al. [14], when studying propane combustion in an autoclave (523–573 K, 0.1–1.5 MPa, $[C_3H_8] = 10$–70% mol.) revealed that at a constant concentration of propane, the self-ignition temperature decreases with increasing pressure. For example, when combusting C_3H_8/air mixture containing 40% of propane, this value decreases from 573 K (0.1 MPa) to 523 K (1.5 MPa).

Wilk et al. [15] studied the low-temperature oxidation of propene in an autoclave (580–715 K, 0.1 MPa, fuel equivalence ratio $\varphi = 0.8$–3.0), determined the range of temperatures corresponding to NTC of the reaction rate, and proposed oxidation mechanisms. It was shown that the initial stage of propene oxidation consists in the hydrogen atom abstraction in the reaction with oxygen

$$CH_3CH=CH_2 + O_2 \rightarrow CH_2CHCH_2 + HO_2. \quad (4)$$

Interaction of HO_2 and OH radicals with propene leads to the formation of allyl radical, hydrogen peroxide, and water

$$CH_3CH=CH_2 + HO_2 \rightarrow CH_2CHCH_2 + H_2O_2, \quad (5)$$

$$CH_3CH=CH_2 + OH \rightarrow CH_2CHCH_2 + H_2O. \quad (6)$$

As a result of the addition of HO_2 to propene in the reaction

$$CH_3CH{=}CH_2 + HO_2 \rightarrow H_3C{-}\underset{\diagdown\,O\,\diagup}{\overset{H}{C}}{-}CH_2 + OH \quad (7)$$

propylene oxide is formed. Based on the analysis of the products composition, the authors [15] concluded that Reactions (5) and (6) are dominant at a temperature of 580–626 K, while the chain branching proceeds mainly through the decomposition of methyl- and allyl-hydroxyperoxide.

Stark and Waddington [16], when studying the low-temperature oxidation of propene in an autoclave (505–549 K, 0.01–0.4 MPa) observed a high yield of propylene oxide. They explained this by reactions involving radicals of HO_2, CH_3O_2, $C_3H_5O_2$, and $C_2H_3CO_3$. From the comparison of experimental data and the proposed kinetic model, the authors [16] concluded that the lower is the temperature, the higher is the yield of propylene oxide; the pressure of the reaction mixture plays a secondary role.

Davis et al. [17] investigated the products composition of the high-temperature ($\approx$1200 K, 0.1 MPa) oxidation and pyrolysis of propene in a flow reactor and proposed DKM of the processes, which include the reactions of the propene, propyne, allene, and propane transformation. Burke et al. [18] investigated numerically and experimentally the combustion of propene using a jet stirred reactor (800–1100 K, 0.1 MPa, $\varphi = 0.6$–2.2) and flow reactor (843–1020 K, 0.6–1.2 MPa, $\varphi = 0.7$–1.3). Using flux and sensitivity analyses, the authors [18] have identified the primary reactions determining the propene combustion rate, namely hydrogen atom abstraction from propene by molecular oxygen, hydroxyl, and hydroperoxyl radicals; allyl-allyl radical recombination; the reaction between allyl and hydroxyperoxyl radicals; and the reactions of 1- and 2-propenyl radicals with molecular oxygen.

Burke et al. [19], when studying combustion of propene by means of the shock tubes and rapid compression machine (750–1750 K, 0.2–4.0 MPa, $\varphi = 0.8$–1.3) showed that the proposed kinetic model is consistent with the experimental data obtained for lean fuel mixtures, however for rich mixtures there was a discrepancy between the kinetic model and experimental data.

Interest in the study of the lower alcohols combustion is caused primarily by the fact that these substances are used as an alternative fuel [20], while isopropanol, in particular, is used as a co-fuel for the disposal of organic waste in supercritical water [21–23]. Li et al. [24] studied the composition of intermediates and combustion products of isopropanol in argon medium (2–4 kPa, $\varphi = 0.75$–1.80) using tunable synchrotron photoionization, and proposed the process mechanisms. It was shown that the loss of hydrogen atom by an isopropanol molecule can occur through the following channels [24]:

$$CH_3CHOHCH_3 + X \rightarrow CH_3COHCH_3 + HX, \quad (8)$$

$$CH_3CHOHCH_3 + X \rightarrow CH_3CHOHCH_2 + HX, \quad (9)$$

$$CH_3CHOHCH_3 + X \rightarrow CH_3CHOCH_3 + HX, \quad (10)$$

where X = H, OH, or CH_3 is some key chain carrier in the system. At that, the abstraction of H atom from CH_3COHCH_3 and

CH_3CHOCH_3 radicals formed in Reactions (8) and (10), respectively, along with the reaction of isopropanol dehydrogenation

$$CH_3CHOHCH_3 \rightarrow (CH_3)_2CO + H_2, \quad (11)$$

leads to the formation of acetone, while the decomposition of $CH_3CHOHCH_2$ radical formed in Reaction (9) and dehydration of isopropanol lead to the formation of propene [24].

Based on the results of a comparative analysis of the composition of propanol and isopropanol combustion intermediates in argon medium (3.3–4.6 kPa, $\varphi = 1.0$–1.9), Kasper et al. [25] concluded that propanol has a greater tendency to soot formation than isopropanol. Frassoldati et al. [26] and Man et al. [27] developed kinetic models of isopropanol oxidation, which showed good agreement with the experimental data obtained by means of the flow reactors and shock tubes at low pressures within a wide range of temperatures (from 900 to 2000 K). Jouzdani et al. [28], when studying isopropanol pyrolysis and combustion (1150–1550 K, 0.3–1.1 MPa, $\varphi = 0.5$–2.0), revealed that at low temperatures, pyrolytic reactions are slower than oxidation reactions, while at high temperatures the reverse trend is observed.

Using experimental and numerical methods, Abdelkhalik et al. [29] determined propane, isopropanol, acetone, and methylacetate ignition regions in the mixtures of fuel/air/CO_2, He, N_2, or Ar at 0.1 MPa. It is shown that the fuel ignition limit depends not only on the concentration of O_2, but also on the chemical structure of the fuel. For example, under the same conditions, the minimum fuel concentration in the mixture at which ignition occurs, increases in the following sequence: $C_3H_8 < C_3H_7OH < C_3H_6O < C_3H_6O_2$.

It is obvious that the combustion is influenced not only by the chemical structure of the fuel, but also by the diluents added to the fuel/O_2 mixture. Ebina et al. [30], when studying the ignition of propane/air/water vapor mixture (0.1 MPa, $[H_2O] \leq 20\%$ wt.), carried out by means of nichrome filament heated by electric current, revealed that the presence of water vapor increases the minimum ignition energy (MIE) for lean fuel mixtures, while for rich mixtures this factor becomes less important. The authors [30] explained this effect by the high heat capacity of water and the involvement of H_2O molecules as a third body in the chain termination reactions at the fuel ignition stage. Using numerical methods, Zhang et al. [31] have shown that for $P \leq 0.1$ MPa, 353 K, and $[H_2O] \leq 15\%$ wt. the MIE value is proportional to the back pressure, and increases exponentially with increasing the dilution level of air-fuel (CH_4 and C_4H_{10}) mixtures with water vapor. In addition, the authors [31] established that the involvement of H_2O molecules in the chain termination reactions significantly increases the MIE value and reduces the limit of mixture dilution by water vapor, in which the fuel ignites. Le Cong et al. [32] studied the influence of water vapor (10% mol.) and carbon dioxide (30% mol.) on combustion of air mixtures of ethylene and propene by means of a jet stirred reactor (950–1450 K, 0.1 MPa, $\varphi = 0.5$–2). It was revealed that H_2O inhibits the oxidation of ethylene, especially in the case of lean fuel mixtures, while CO_2 slightly accelerates oxidation. No effects of H_2O and CO_2 on the oxidation of propene were noted in [32]. Lubrano Lavadera et al. [33], when studying the effect of water vapor on the combustion of propane in nitrogen medium (jet stirred flow reactor, 720–1100 K, 0.11 MPa, $\varphi = 0.5$–1.5, $[H_2O] \leq 40.5\%$ mol.) have revealed that at low temperature, water as a third body is actively involved in the hydrogen peroxide decomposition

$$H_2O_2 + M \rightarrow OH + OH + M, \quad (12)$$

that accelerates the oxidation. Holgate and Tester [34] in the study of the hydrogen oxidation kinetics in supercritical water (flow reactor, 678–873 K, 24.6 MPa) have found that the rate of the chain-branching reaction

$$HO_2 + H_2O \rightarrow H_2O_2 + OH, \quad (13)$$

increases along with the increase in the water density.

Sabia et al. [35] studied the effect of H_2O and CO_2 on the ignition of propane/air mixture using experimental (flow reactor, 850–1250 K, 0.1 MPa) and numerical methods. It was revealed that H_2O and CO_2 have both thermal and chemical effects on the reactivity of the mixture. The authors [35] explained these effects by the high heat capacity of H_2O and CO_2, which cause a decrease in the temperature of the adiabatic flame that in turn leads to a change in the kinetic channels of the reactions. One of such channels influencing the direction of fuels oxidation, according to [36,37], is the involvement of carbon dioxide in the reaction

$$CO_2 + H \leftrightarrow CO + OH. \quad (14)$$

Data on the oxidation of propane and propene in supercritical water, available in the literature, were not found. At the same time, the kinetics and mechanisms of supercritical water oxidation (SCWO) of isopropanol are well studied [21,38,39]. Hunger et al. [38], when studying SCWO of isopropanol (673–753 K, 24.5 MPa, oxygen excess 15%), established that acetone is the main oxidation intermediate. Krajnc and Levec [39] studied SCWO of isopropanol in a flow tubular reactor (658 K, 23.3 MPa, oxygen excess 135%) at a holding time of 15–30 s. Abelleira et al. [21] conducted an experimental study (673–773 K, 25 MPa, oxygen excess 50–100%) and numerical simulation of the SCWO kinetics of isopropanol. The proposed kinetic model [21], which is in good agreement with the experimental data, is based on a two-stage SCWO process: the first fast stage corresponds to the oxidation of isopropanol and acetone, while the second slow stage corresponds to the oxidation of acetic acid, acetaldehyde, and formaldehyde.

It follows from the above analysis that data on the effects of H_2O and CO_2 on the ignition of C_3-fuels at elevated pressures and low temperatures, as well as on the composition of their partial oxidation products, are fragmented. In this paper, the effect of H_2O and CO_2 on the oxidation of propane, propene, and isopropanol under high density of the reagents at their uniform slow heating is studied for the first time. Unlike water and carbon dioxide, argon is a chemically inert diluent, which will allow revealing the role of H_2O and CO_2 in the oxidation of C_3 fuels.

2. Experimental procedures

The schematic diagram of the experimental setup is described in detail in [6–8]. The main element of the setup is a tubular reactor (internal diameter 30 mm, volume 65.0 cm^3), made of stainless steel AISI 321. The reactor was placed in a furnace, whose temperature was controlled by temperature programmer conjugated with thermocouple (T_{out}), installed at the outer wall of the reactor. The reactants temperature was measured by internal thermocouple (T_{in}), introduced to the center of the reaction volume through the end face of the reactor. The accuracy of temperature measurement was ±0.5 K. Pressure of the reagents was measured by the membrane strain gauge. The accuracy of the pressure measurement was 0.15% of the measured value. Time dependences of the temperature and pressure were recorded in the digital form with a frequency of 10 Hz using analogue-to-digital converter. Reagents were fed to the previously evacuated reactor through a capillary welded into the central part of the reactor sidewall (along the horizontal plane passing through the reactor axis) through the adjusting valve. The volume of the reactor inside the furnace was 64.1 cm^3, while those of the cold volumes outside the furnace were 0.9 cm^3. Before each

Table 1
Experimental conditions and results.

Test (Fuel)	Partial pressure of components (MPa)			Amount of components (mmol)			φ	x_d (% mol.)	α_f (% mol.)	α_O (% mol.)
	Fuel	O_2	Diluent	$[Fuel]_0$	$[O_2]_0$	$[Diluent]_0$				
Argon										
1 (C_3H_8)	0.51	2.19	3.82	14.2	56.6	101	1.25	59	97.3	99.0
2 (C_3H_6)	0.55	1.95	4.06	15.4	50.8	107	1.36	62	88.2	87.8
3 (C_3H_7OH)	–	1.99	4.03	15.7 (10.9)[a]	50.4	103	1.40	61	99.8	97.5
Carbon dioxide										
4 (C_3H_8)	0.56	2.18	3.35	15.7	56.5	101 (15.8)	1.39	58	74.6	97.4
5 (C_3H_6)	0.54	1.94	3.32	15.0	50.5	101 (15.8)	1.34	61	70.6	57.1
6 (C_3H_7OH)	–	1.98	3.37	15.7 (10.9)	50.4	103	1.40	61	99.8	98.0
Water vapor										
7 (C_3H_8)	0.57	2.16	–	15.2	52.9	103	1.44	60	98.0	99.1
8 (C_3H_6)	0.55	1.96	–	14.9	49.0	103	1.37	62	–	–
9 (C_3H_7OH)	–	2.10	–	15.7	51.5	103	1.37	61	–	–
10 (C_3H_8)	0.56	2.27	–	15.2	56.8	172	1.34	70	94.8	94.6
11 (C_3H_6)	0.59	2.15	–	15.8	52.8	172	1.35	71	87.5	98.5
12 (C_3H_7OH)	–	2.09	–	15.7	50.2	172	1.41	72	95.0	98.2

[a] The amount of isopropanol and carbon dioxide condensed in the cold volumes of the reactor is given in brackets; their amount in the hot part of the reactor is indicated before the brackets.

test, the internal surface of the reactor was passivated (oxidized) with H_2O/O_2 at 873 K. Each test was repeated 2–3 times.

Twelve tests were conducted for different compositions of the reaction mixtures (Table 1). In tests 1–3 argon was used as a diluent of fuel/O_2 mixture, in tests 4–6 – carbon dioxide, and in tests 7–12 – water vapor. In tests 1, 2 and 4, 5, where propane and propene were used as a fuel, respectively, the reaction mixture components were charged to the reactor at 303 K to a given pressure in the following sequence: diluent (to a pressure of ≈ 0.30 MPa), fuel, diluent, and oxygen. Such reactor charging sequence is, on the one hand, due to the need to fill the cold volumes with a diluent to reduce the error in determining the amount of fuel in the heated part of the reactor, and on the other hand, by the low pressure of saturated vapor of propane and propene in a standard cylinder (0.83 and 1.02 MPa, respectively, at 293 K [40]).

In tests 3 and 6, where isopropanol was used as a fuel, the non-heated volumes of the reactor were filled with isopropanol before supplying the diluent and oxygen. To do this, the reactor was fed with isopropanol in amount of 2.1 cm^3 injected using syringe through the rubber diaphragm installed on the connecting branch of the reagent flow valve. Then the reactor was heated up to $T_{out} = 383$ K (isopropanol boiling temperature is equal to 355 K [41]) and held at this temperature for 45 min. At that, some isopropanol (≈ 0.9 cm^3) was condensed in the cold volumes and 15.7 mmol of isopropanol (its density at 293 K is 0.786 g/cm^3 [41]) remained in the heated part of the reactor. After cooling the reactor to 303 K, it was successively charged with diluent (Ar or CO_2) and oxygen to a predetermined pressure.

In tests 7, 8 and 10, 11, where propane and propene were used as a fuel, 2.8 and 4.0 cm^3, respectively, of distilled water was filled into the reactor through the separation membrane at room temperature. The reactor was then heated to $T_{out} = 403$ K and thermostated for 45 min. During this time, the cold volumes of the reactor were filled with water. After thermostating the reactor, 103 mmol (tests 7, 8) and 172 mmol (tests 10, 11) of water remained in its heated part. After cooling to 303 K the reactor was successively charged with fuel (propane or propene) and oxygen.

In tests 9 and 12, where isopropanol was used as a fuel, the reactor charging procedure was as follows. To fill the cold volumes with water, the reactor was charged with 1.8 and 3.0 cm^3 of distilled water, respectively, then the reactor was heated to $T_{out} = 403$ K and thermostated similarly to tests 7, 8, 10, and 11. After cooling the reactor to 303 K, it was successively charged with 1.2 cm^3 of isopropanol, 1.0 cm^3 of distilled water, and oxygen to a predetermined pressure.

After charging the reagents, the reactor was heated at the rate $q = 1$ K/min to a set temperature. Table 1 shows the partial pressure of reagents and diluents fed to the reactor, their amount ($[Fuel]_0$, $[O_2]_0$, and $[Diluent]_0$) in the heated part of the reactor, the fuel equivalence ratio φ, the dilution level x_d of the mixture, the conversion degree of fuel α_f and oxygen α_O. The amounts of reagents and diluents were determined based on their temperature and partial pressure, as well as reactor volume using the reference P–ρ–T data [40].

After reaching the set temperature, the reactor was cooled at a rate of ≈ 6 K/min to room temperature, and the residual pressure of the reactants in the reactor was measured. The composition and amounts of volatile reactants were determined using quadruple mass spectrometer MS-7303 according to the method [42]. The sampling of volatile products for analysis was carried out through the capillary feeder [6–8]. The amount of carbon in the soot composition as well as low-volatile liquid products, found in the reactor after analysis of volatile reactants in tests 1–6, were determined as follows. The reactor was charged with water (≈ 200 mmol) and oxygen (≈ 25 mmol), heated to 873 K and kept at this temperature for 60 minutes. After cooling the reactor to room temperature, mass-spectrometric analysis of volatile products was carried out. The results of the conducted analysis were used to determine the amount of $(CO_2)_R$ and the corresponding amount of carbon. During the oxidation of fuels in the H_2O medium (tests 7–12), no soot and low-volatile liquid products were detected.

3. Experimental results

Oxidation of propane, propene, and isopropanol by oxygen is described by the following gross-reactions:

$$C_3H_8 + 5O_2 = 3CO_2 + 4H_2O, \quad \Delta H°_{298} = -2044\ \text{kJ/mol}, \quad (15)$$

$$C_3H_6 + 4.5O_2 = 3CO_2 + 3H_2O, \quad \Delta H°_{298} = -1886\ \text{kJ/mol}, \quad (16)$$

$$C_3H_7OH + 4.5O_2 = 3CO_2 + 4H_2O, \quad \Delta H°_{298} = -1875\ \text{kJ/mol}. \quad (17)$$

In this paper, we investigated the oxidation features of high-density C_3H_8/O_2, C_3H_6/O_2, and C_3H_7OH/O_2 mixtures diluted with argon (tests 1–3), carbon dioxide (tests 4–6), and water vapor (tests 7–12). As is obvious from Table 1, tests were carried out with fuel-enriched mixtures ($\varphi = 1.25$–1.44) at their dilution level x_d ranged from 59 to 72% mol.

Table 2
Characteristic points of curves in Figs. 1–5 and the thermodynamic parameters of the reaction mixtures.

Test (Fuel)	T_{out}^* (K)	T_{in}^* (K)	T_{out}^{min} (K)	T_{in}^{min} (K)	t_{ox} (min)	S (K·min)	T_{out}^{max} (K)	T_{in}^{max} (K)	ΔT^{max} (K)	C_v^* (J/K)	ΔT_{ad}^* (K)
Argon											
1 (C_3H_8)	522	518	562	557	40	202	543	1290	751	4.1	5634
2 (C_3H_6)	473	465	565	560	90	185	497	507	18	3.8	5605
3 (C_3H_7OH)	482	477	580	572	98	259	568	1133	570	4.3	4883
Carbon dioxide											
4 (C_3H_8)	524	519	626	622	102	692	544	554	16	6.8	3397
5 (C_3H_6)	472	466	516	512	44	166	493	503	16	6.0	3528
6 (C_3H_7OH)	508	503	574	568	66	297	563	922	364	6.9	3043
Water vapor											
7 (C_3H_8)	524	522	580	578	56	219	569	1345	778	5.8	3729
8 (C_3H_6)	471	465	603	600	132	358	590	595	11	3.2	6418
9 (C_3H_7OH)	532	528	621	620	89	141	609	613	7	7.0	3065
10 (C_3H_8)	525	523	616	616	91	202	583	674	93	6.0	3870
11 (C_3H_6)	471	465	596	593	125	279	504	507	9	3.1	7138
12 (C_3H_7OH)	532	528	628	624	96	134	615	616	5	6.9	3031

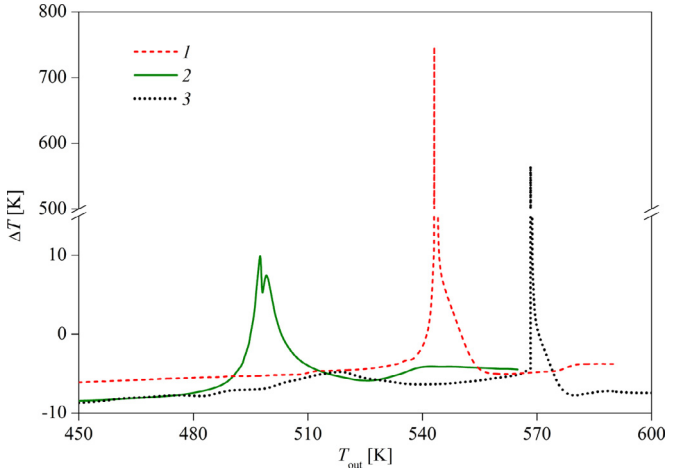

Fig. 1. Temperature dependences of difference in temperature ($\Delta T = T_{in} - T_{out}$) of reactants in the center of the reactor (T_{in}) and the external reactor wall (T_{out}) during propane (*1*), propene (*2*), and isopropanol (*3*) oxidation in the argon medium. Numbers of the curves correspond to numbers of tests in Table 1.

3.1. Argon as a diluent

Figure 1 presents the temperature difference $\Delta T = T_{in} - T_{out}$ versus T_{out} during the oxidation of fuels in the argon medium (tests 1–3). Here and below T_{out} corresponds to a given increase in the reactor wall temperature at the rate $q = 1$ K/min, and T_{in} is the reactant temperature, measured using the internal thermocouple. As can be seen, against the background of an increase in $T_{out}(t)$, a temperature increment $\Delta T(t)$, caused by self-ignition of fuel/O_2 mixture (self-acceleration of exothermic Reactions (15)–(17)), was observed in all the tests.

Table 2 shows the following parameters of the curves $\Delta T(T_{out})$ and the reaction mixtures. Here T_{out}^* and T_{in}^* are the reactor wall temperature and the reaction mixture temperature, respectively, corresponding to occurrence of self-ignition. These values are defined from the condition

$$\left|\Delta T_i(T_{out}) - \Delta T'_i(T_{out})\right| > 3\sigma, \tag{18}$$

where $\sigma = \{[\sum(\Delta T_i(T_{out}) - \Delta T_i'(T_{out}))^2]/(n-1)\}^{0.5}$ is the standard deviation of experimentally measured values on the linear portion of the curve $\Delta T(T_{out})$ before oxidation. Temperatures T_{out}^{min} and T_{in}^{min} correspond to the end of fuels oxidation and cooling of the reaction mixture to a predetermined temperature T_{out} (correspond to the minimum of the curve $\Delta T(T_{out})$). The oxidation duration is calculated by the formula

$$t_{ox} = (T_{out}^{min} - T_{out}^*)/q \tag{19}$$

The area S under the curve $\Delta T(T_{out})$ confined by baseline corresponds to time t_{ox}. Here, the baseline is a straight line connecting the straight sections of the $\Delta T(T_{out})$ dependence before and after oxidation. Temperatures T_{out}^{max} and T_{in}^{max} correspond to the maximum of the curve $\Delta T(T_{out})$. The maximum increment of the reaction mixture temperature resulting from heat released during combustion is calculated by the formula

$$\Delta T^{max} = (T_{in}^{max} - T_{in}^*) - (T_{out}^{max} - T_{out}^*). \tag{20}$$

The heat capacity of the reaction mixture at a temperature T_{in}^* is determined by the formula

$$C_v^* = \Sigma C_{v,i} x_i, \tag{21}$$

using the reference data [40]. Here x_i is the molar fraction of the i-th component in the gas phase. The temperature increment of the reaction mixture in adiabatic conditions due to heat release in Reactions (15)–(17) is calculated by the formula

$$\Delta T_{ad}^* = Q/C_v^*. \tag{22}$$

We believe that heat release during fuels oxidation in the context of the present work occurs due to both homogeneous (in the volume of the reaction mixture) and heterogeneous (at the reactor wall) reactions. The heterogeneous exothermic reactions almost do not affect the indications of the thermocouple T_{in} due to the high heat capacity $C = 548$ J/kg·K and the thermal conductivity $\lambda = 21$ W/m·K of stainless steel [43], as well as the stabilizing effect of the thermal programmer, which regulates the reactor heating by reducing the heater power. Under adiabatic conditions, heat release at complete oxygen consumption in tests 1, 2, and 3 ($Q = 23.1$, 21.3, and 21.0 kJ) could have led to an increase in the reactor temperature, whose mass was 3.6 kg, by ≈ 11 K, or the gas contained in the reactor ($C_v^* = 4.1$, 3.8, and 4.3 J/K), at homogeneous combustion – by $\Delta T_{ad}^* = 5634$, 5605, and 4883 K (Table 2). In fact, the temperature increment of the reaction mixture ΔT^{max} turned out to be significantly less than ΔT_{ad}^* due to the heat removal from the reaction system.

As is obvious from Table 2, the self-ignition temperature T_{in}^* of fuels in the Ar medium increases in the following sequence: $C_3H_6 < C_3H_7OH < C_3H_8$ that corresponds to the change in the energy of the H atom abstraction from the fuel molecule (360, 380, and 410 kJ/mol [44], respectively). Note that the propane self-ignition temperature $T_{in}^* = 518$ K, observed in this paper, was close to the same value obtained by Norman et al. [14] in the study of combustion of propane/air mixtures.

Table 3
Composition and amounts of the products of fuels oxidation in the argon, carbon dioxide, and water vapor media (mmol).

Products	Argon			Carbon dioxide			Water vapor			
	1 (C_3H_8)	2 (C_3H_6)	3 (C_3H_7OH)	4 (C_3H_8)	5 (C_3H_6)	6 (C_3H_7OH)	7 (C_3H_8)	10 (C_3H_8)	11 (C_3H_6)	12 (C_3H_7OH)
Ar	100.4	106.6	103.1	–	–	–	–	–	–	–
H_2	15.06	0.71	48.97	0.86	0.77	2.84	31.1	3.09	1.12	3.28
O_2	0.56	6.11	1.25	1.45	21.65	1.00	0.45	3.07	0.78	0.89
CO	8.22	3.66	27.57	5.38	5.76	17.77	2.36	0.83	3.66	3.14
CO_2	28.22	18.05	22.73	127.9	117.5	125.5	39.3	40.1	31.84	30.04
Methane	0.05	0.27	14.60	0.58	0.12	19.06	0.33	0.50	0	0.09
Methanol	0	2.12	0.02	1.70	1.82	0.22	0.03	0.13	0.19	0.46
Formaldehyde	0.05	0.22	0.05	0.20	0.41	0.11	0.16	0.02	0	0.01
Formic acid	0	0.01	0.02	0.02	0	0	0.16	0.02	0	0.01
Ethane	0.02	0.12	0.13	0.12	0.12	1.57	0.06	0.13	0	0.04
Ethylene	0	0	0.02	0.11	0.01	0.57	0.13	0.03	0	0.02
Ethanol	0	0.13	0.02	0.06	0.24	0.12	0	0.02	0.01	0.02
Acetaldehyde	0	0.56	0.05	0.73	0.93	0.59	0.05	0.13	0.05	0.30
Acetic acid	0.03	0.44	0.27	0.05	0.50	0.44	0.16	0.04	0.01	0.18
Propane	0.38	0.13	0.01	3.98	0.08	0.05	0.31	0.79	0	0
Propene	0	1.82	0.07	0	4.41	0.48	0	0.07	1.98	0.50
Isopropanol	0	0	0.04	0	0	0.04	0	0	0	0.78
Acetone	0	0.82	0.33	0.53	0.65	2.22	0	0.03	0.02	0.77
Propylene oxide	0.03	0.01	0.44	0	0.02	0	0	0	0	0
Propylene carbonate	–	–	–	–	0.03	–	–	–	–	–
Butadiene	0.05	0.02	0.03	0.01	0.03	0.06	0	0	0.01	0
$(CO_2)_R$	2.02	7.45	9.92	3.36	8.26	3.49	–	–	–	–
Carbon balance (% mol.)	94.1	92.4	98.6	94.5	94.7	99.2	96.7	98.7	88.3	87.1

The carbon balance is given considering the amount of isopropanol and carbon dioxide condensed in the cold volumes of the reactor.

In Fig. 1, it can be seen that a noticeable increase in the rate of $d\Delta T/dT_{out}$ in the oxidation of propane (curve *1*) began at a temperature lower than that in the oxidation of isopropanol (curve *3*). According to the reference data [41], complete evaporation of isopropanol in test 3 occurred at $T_{ev} = 422$ K, that is, at the time of self-ignition ($T^*_{in} = 477$ K), all isopropanol was in the gas phase. Therefore, an increase in the temperature corresponding to the onset of intense oxidation of isopropanol can be caused by both a greater heat capacity of the $C_3H_7OH/O_2/Ar$ mixture (Table 2) and chemical transformations of isopropanol. Oxidation of isopropanol occurs in two stages with the maxima at $T^{max}_{out} = 518$ and 568 K (Fig. 1). Since at $T > 355$ K isopropanol is subjected to dehydrogenation (see Reaction (11)) with the formation of acetone and hydrogen [45], it can be assumed that the second stage corresponds to the oxidation of the products of Reaction (11).

As seen in Fig. 1, the oxidation of propane (curve *1*) and isopropanol (curve *3*) was accompanied by chain-thermal explosion. According to Semenov [46] and Frank-Kamenetskii [47], such a regime is implemented at avalanche-like reproduction of atoms and radicals, as well as if the heat release from the chemical reaction prevails over the heat removal; with an increase in temperature, heat release accelerates to a greater extent than the heat removal. As a result of the chain-thermal explosion during the oxidation of propane and isopropanol, the temperature increment ΔT^{max} amounted to 751 and 570 K, and the temperature of the reaction mixture reached 1290 and 1131 K, respectively (Table 2). Sharp decrease of $\Delta T(T_{out})$ on curves *1* and *3* (Fig. 1) at $T_{out} > T^{max}_{out}$ is caused by the depletion of O_2 and the heat removal, while the presence of a minimum on these curves is a consequence of the response delay of the reactor heating control system. The area *S* characterizing the heat release, in the oxidation of isopropanol (test 3) was slightly larger than that in the oxidation of propane (test 1), despite the greater amount of $[O_2]_0$ in test 1 comparing to test 3 (Table 1), and a greater thermal effect of Reaction (15) comparing to Reaction (17). Obviously, this is a consequence of a greater heat removal in the oxidation of propane due to a greater increment in temperature ΔT^{max} and a longer oxidation time t_{ox} of isopropanol (Table 2).

No chain-thermal explosion was observed in the propene oxidation. According to Semenov [46], type of curve *2* observed in Fig. 1 corresponds to the degenerate explosion. The maximum temperature increment ΔT^{max} during the propene oxidation was just 18 K; at that, the area *S* was only slightly less than that in the propane oxidation (Table 2). We explain this fact by the formation of low-volatile liquid products, whose oxidation rate is lower than the gas-phase oxidation rate. We have previously established [11] that at uniform heating (1 K/min) propene is subjected to oligomerization at $T \geq 587$ K with the formation of a wide range of aromatic hydrocarbons. Apparently, the above processes also took place under the conditions of the present work as evidenced by the high values of $(CO_2)_R$ (Table 3).

The results of mass spectrometric analysis of the composition and quantity of propane, propene, and isopropanol oxidation products are given in Table 3. The fuel and oxygen conversion degree calculated from these data are given in Table 1. As can be seen, at the oxidation of propane and isopropanol, values of α_f and α_O are close to 100% due to the high values of T^{max}_{in} (Table 2). However, unlike propane, whose oxidation products are dominated by CO_2, the isopropanol oxidation was accompanied by intense pyrolysis, as indicated by a high yield of H_2, CO, and CH_4 (test 3, Table 3). This is consistent with the conclusion of Jouzdani et al. [28] about a higher rate of pyrolytic reactions than oxidation reactions at high temperature. Using computational chemistry calculations, Biu et al. [48] stated that at high-pressure and temperature over 1000 K, direct C–C bond scission to produce CH_3 and $CH_3C(H)OH$ becomes dominant that leads to a high yield of CO and CH_4 in isopropanol pyrolysis.

Another source of CO in the conditions of the present work can be the decomposition of CO_2. Considering the data of Zhang et al. [49], it can be assumed that the oxide layer on the internal surface of the reactor, whose main component is magnetite Fe_3O_4 [50], catalytically influenced the decomposition of CO_2. According to the

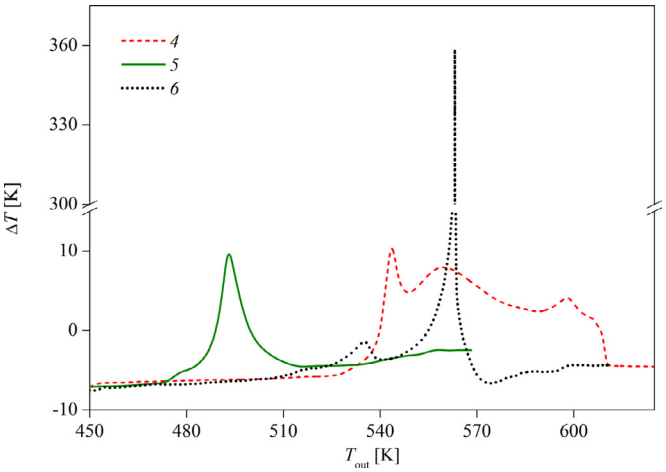

Fig. 2. Temperature dependences of difference in temperature ($\Delta T = T_{in} - T_{out}$) of reactants in the center of the reactor (T_{in}) and the external reactor wall (T_{out}) during propane (*4*), propene (*5*), and isopropanol (*6*) oxidation in the carbon dioxide medium. Numbers of the curves correspond to numbers of tests in Table 1.

mechanisms proposed by Zhang et al. [49], decomposition of CO_2 on oxygen-deficient $Fe_3O_{4-\varepsilon}$ ($\varepsilon > 0$) proceeds in two stages:

$$CO_2 \rightarrow CO + O^{2-} \text{ and } CO \rightarrow C + O. \quad (23)$$

Based on the fact that the self-ignition temperature T_{in}^* of hydrogen in the N_2 medium is ≈ 510 K [6], such a high yield of H_2 during the oxidation of isopropanol in the Ar medium (Table 3) is a hard-to-explain fact. We assumed that this is due to the predominant oxidation of hydrocarbon radicals and the lack of O_2 (Table 1). Note that the self-ignition temperature of methane T_{in}^* in the N_2 medium is equal to 639 K [7], which is significantly higher than the oxidation end temperature T_{in}^{min} of isopropanol (Table 2). In general, the data on the product composition of partial oxidation of propane and isopropanol are consistent with the results [12,13,24–28].

In contrast to propane and isopropanol, propene was less oxidized (see α_f and α_O in Table 1) that is caused by both a lower temperature increment ΔT^{max} (Table 2) and the formation of low-boiling substances resulting from its oligomerization [11]. Table 3 shows that besides CO and CO_2, the substances such as methanol, acetone, acetaldehyde, and acetic acid, which are produced through propene partial oxidation, are observed in significant amounts that is consistent with the results [15,16].

It follows from the obtained results that the oxidation of C_3H_8 and C_3H_7OH in the Ar medium proceeds through the chain-thermal explosion mechanism and leads to almost complete fuel conversion and O_2 consumption. The oxidation of C_3H_7OH is accompanied by intense thermolysis with the formation of H_2, CH_4, and CO. The implementation of chain-thermal explosion in the oxidation of C_3H_6, apparently, prevents the formation of low-boiling substances due to its oligomerization.

3.2. Carbon dioxide as a diluent

Figure 2 presents the temperature difference $\Delta T = T_{in} - T_{out}$ versus T_{out} during the oxidation of fuels in the carbon dioxide medium (tests 4–6). It is seen that the oxidation of isopropanol (curve *6*) proceeds through the chain-thermal explosion mechanism, while the oxidation of propane (curve *4*) and propene (curve *5*) corresponds to the degenerate explosion [46]. The self-ignition temperature T_{in}^* of propane and propene in CO_2 medium (tests 4 and 5) is almost similar to values obtained in the Ar medium (tests 1 and 2), despite the large heat capacity of $C_3H_8/O_2/CO_2$ and $C_3H_6/O_2/CO_2$ mixtures (Table 2). However, the self-ignition temperature of isopropanol in CO_2 medium (test 6) was by 26 K higher than that in Ar medium (test 3). The chain-thermal explosion and the increase in T_{in}^* at the isopropanol oxidation in the CO_2 medium is, apparently, a consequence of the predominant combustion of H_2 formed during Reaction (11). This is indicated by a 17-fold decrease in the yield of H_2 and an increase in the yield of products of partial oxidation (acetaldehyde, acetone, and acetic acid) and pyrolysis (methane, ethane, ethylene, and propene) of isopropanol compared to test 3 (Table 3), as well as data on the combustion of H_2 in the N_2 and CO_2 media [6]. We have previously established [6] that the self-ignition temperature of the $H_2/O_2/N_2$ mixture is by ≈ 30 K lower than that of the $H_2/O_2/CO_2$ mixture; at that, the oxidation of H_2 in the CO_2 medium proceeds through the mechanism of chain-thermal explosion, which is not observed in the N_2 medium.

These peculiarities of hydrogen oxidation in the high-density CO_2 medium are explained by the formation of van der Waals complexes involving CO_2 molecules and radicals, mainly, HO_2 and OH. According to quantum-chemical calculations carried out by Masunov et al. [37], the formation of such complexes contributes to the stabilization of the transition state and lowering the activation barrier of reactions. In particular, it is shown [37] that the formation of van der Waals complexes in the reaction

$$CO + OH + CO_2 \rightarrow CO + [CO_2 \cdots OH] \rightarrow 2CO_2 + H, \quad (24)$$

reduces its activation barrier by ≈ 21 kJ/mol compared to bimolecular Reaction (14).

As a result of the chain-thermal explosion during the isopropanol oxidation in CO_2 medium, the temperature increment ΔT^{max} was by 206 K lower than that in Ar medium (Table 2), despite the same amount of charged reagents in tests 3 and 6 (Table 1). As can be seen in Figs. 1 and 2, the oxidation of isopropanol in CO_2 medium, similar to oxidation in Ar medium, proceeds in two stages with the maxima at $T_{out}^{max} = 535$ and 563 K. However, the duration of oxidation t_{ox} in CO_2 medium was by ≈ 1.5 times less than that in Ar medium, at slightly different *S* values (Table 2). In general, the conversion degree α_f and α_O at the isopropanol oxidation in CO_2 medium was close to 100% (Table 1).

It can be seen in Figs. 1 and 2 that in CO_2 medium (curve 5), a noticeable increase in the oxidation rate $d\Delta T/dT_{out}$ of propene started at a slightly lower temperature as compared to that in Ar medium (curve *2*). This may be resulted from both chemical interaction in the $C_3H_6/O_2/CO_2$ mixture and shielding of the reactor internal surface by adsorbed CO_2 molecules, leading to a decrease in the contribution of heterogeneous exothermic reactions, and as a consequence, reducing the heat removal from the reaction system. We have earlier considered in detail the effect of adsorbed diluent molecules on the contribution of homogeneous and heterogeneous reactions to the measurable heat release on the example of H_2 oxidation [6]. The maximum temperature increment ΔT^{max} during the oxidation of propene in CO_2 medium was slightly less than that in Ar medium that may be due to the greater heat capacity of the $C_3H_6/O_2/CO_2$ mixture (Table 2). At that, the values of the area *S* during the propene oxidation in the Ar and CO_2 media are approximately equal.

As is obvious from Table 1, the conversion degree of propene and oxygen in CO_2 medium was minimal (70.6 and 57.1% mol., respectively). One of the reasons for this may be the formation of propylene carbonate (Table 3) in the interaction of propylene oxide formed in Reaction (7) with carbon dioxide [51,52]

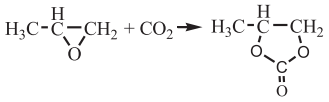

(25)

Based on the fact that propylene carbonate, unlike propylene oxide, has a lower saturated vapor pressure (boiling point is 513 and 308 K, respectively [41]), and the rate of liquid-phase oxidation is less than that of gas-phase, we can conclude that the formation of propylene carbonate in Reaction (25) and the formation of low-boiling substances, resulted from propene oligomerization [11], prevented the development of intense fuel oxidation in the CO_2 medium.

Propane oxidation in CO_2 medium (test 4) is characterized by a wide temperature range of the process and the presence of three maxima on the $\Delta T(T_{out})$ curve at T_{out}^{max} = 543, 560, and 598 K (Fig. 2). At that, the maximum at 543 K coincides with the temperature T_{out}^{max} recorded during the oxidation of propane in Ar medium (test 1, Table 2). The duration of oxidation t_{ox} in the CO_2 medium and the area S were respectively by 2.5 and 3.4 times greater than in the Ar medium, while the maximum temperature increment ΔT^{max} in the CO_2 medium was only 16 K. As a result, with almost complete consumption of O_2 (α_O = 97.4% mol.) the degree of propane conversion in CO_2 medium (test 4) was only 74.6% mol. (Table 1). Methanol, acetaldehyde, and acetone were detected in the composition of propane oxidation products in significant amounts, which was not observed during its oxidation in Ar medium due to a larger temperature increment ΔT^{max} (Tables 2 and 3).

We believe that a low degree of propane conversion at such a long process duration, as well as the failure of the explosive oxidation regime in the CO_2 medium, are due to the combination of high density of CO_2 in the reaction mixture and the presence of resonance exchange of vibrational energy (V–V exchange) [53] between C_3H_8 and CO_2 molecules:

$$C_3H_8^*(\nu_j = 1392,\ 1378\ cm^{-1}) + CO_2 \leftrightarrow C_3H_8 + CO_2^*(\nu_1 = 1388\ cm^{-1}), \quad (26)$$

$$C_3H_8^*(\nu_j = 1338\ cm^{-1}) + 2CO_2 \leftrightarrow \leftrightarrow C_3H_8 + CO_2^*(\nu_2 = 667\ cm^{-1}) + CO_2^*(\nu_2 = 667\ cm^{-1}), \quad (27)$$

$$CO_2^*(\nu_1 = 1388\ cm^{-1}) + CO_2 \leftrightarrow CO_2^*(\nu_2 = 667\ cm^{-1}) + CO_2^*(\nu_2 = 667\ cm^{-1}), \quad (28)$$

where ν_j = 1392, 1378, and 1338 cm^{-1} correspond to the deformation oscillations of CH_3, CH_2, and CH_2 groups; ν_1 and ν_2 are stretching frequencies of symmetric and deformation oscillations of the CO_2 molecule, respectively [54]. Consequently, the avalanche reproduction of radicals, which is necessary to realize chain-thermal explosion, according to Semenov [46] and Frank-Kamenetskii [47], was prevented by the deactivation of vibrationally excited molecules of $C_3H_8^*$ in Reactions (26) and (27), as well as the energy sink of vibrational excitation of $CO_2^*(\nu_2 = 667\ cm^{-1})$ to the reactor wall. High speed of the vibrational energy transport to the rector wall due to V–V exchange is ensured by the high density of CO_2, while the high rate of subsequent deactivation of the $CO_2^*(\nu_2 = 667\ cm^{-1})$ molecules is caused by the presence of adsorbed layer of CO_2 molecules on the reactor wall [6]. The mechanisms of increasing the rate of deactivation of CO_2^* molecules in their collision with the condensed phase are described in [55]. Since the deformation frequencies of CH_3 and CH_2 groups in propane and propene are close to each other [54], it can be assumed that the resonance V–V exchange in the C_3H_6/CO_2 mixture also influenced the propene oxidation, which contributed to its low degree of conversion. Note that a similar effect was observed in the study of isobutane oxidation in CO_2 medium [8].

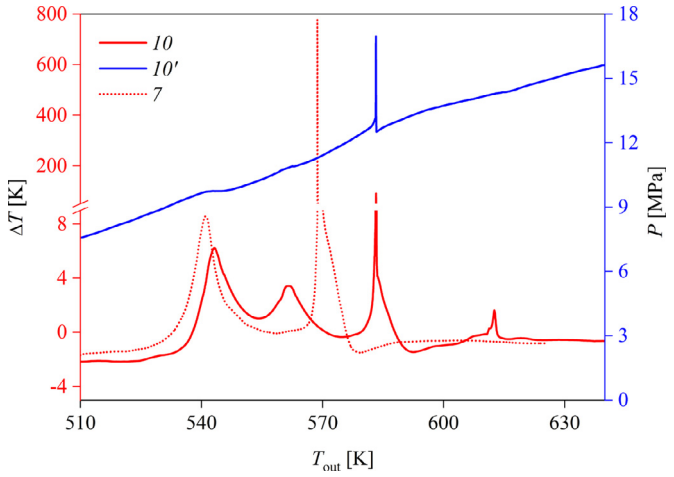

Fig. 3. Temperature dependences of difference in temperature ($\Delta T = T_{in} - T_{out}$) of reactants in the center of the reactor (T_{in}) and the external reactor wall (T_{out}), as well as pressure (P) of the reaction mixtures during propane oxidation in water vapor at the dilution level of 60 (*7*) and 70% mol. (*10*, *10′*). Numbers of the curves correspond to numbers of tests in Table 1.

From the results obtained, it follows that the oxidation of C_3H_7OH in CO_2 medium proceeds according to the chain-thermal explosion mechanism and leads to almost complete conversion of fuel and consumption of O_2, similarly as in the oxidation in Ar medium. The oxidation of C_3H_8 in CO_2 medium is characterized by a low degree of fuel conversion with almost complete consumption of O_2, while the oxidation of C_3H_6 is characterized by both a low degree of fuel conversion and consumption of O_2.

3.3. Water vapor as a diluent

The results of time-dependent measurements of T_{out}, T_{in}, and pressure P of the reaction mixture obtained during the fuels oxidation in water vapor (tests 7–12) are shown in Figs. 3–5 in the form of $\Delta T(T_{out})$ and $P(T_{out})$ dependencies. Compared with tests 7–9, the amount of water $[H_2O]_0$, charged into the reactor (Table 1) in tests 10–12 was increased by 1.7 times. According to the reference data [40], complete evaporation of water in the reaction system in tests 7–9 and 10–12 occurred at T_{ev} = 545 and 576 K, respectively. Based on the fact that the self-ignition temperature of propane, propene, and isopropanol $T_{in}^* < T_{ev}$ (Table 2), it follows that their oxidation was accompanied by evaporation of water, that is, an increase in the heat capacity and thermal conductivity of the reaction medium with the increase in temperature (Fig. 6). At the same time, certain portion of the heat released during the oxidation of fuel, was spent on the evaporation of water. For example, in tests 7 and 8, the thermal inputs on evaporation of water at the temperature increase from T_{in}^* to T_{ev} are 1.7 and 4.0 kJ [40], which corresponds to the amount of heat released during the oxidation of 0.8 and 3.4 mmol of propane and propene, respectively (see Reactions (15) and (16)). The behavior of $P(T_{out})$ curves in Figs. 3–5 corresponds to the pressure change associated with the water evaporation with the increase in temperature, the heat release during the oxidation of the fuel, and cooling of the reaction mixture to a predetermined temperature of T_{out}.

As follows from the data given in Table 2, the self-ignition temperature T_{in}^* of propane in H_2O medium (test 7) turned out to be by 3–4 K higher than that in Ar and CO_2 media (tests 1 and 4). Note that this value T_{in}^* was close to the self-ignition temperature of isobutane obtained under similar conditions [8]. From Fig. 3 it

is clear that the propane oxidation in H_2O medium occurs according to the chain-thermal explosion mechanism, similar to oxidation in Ar medium (Fig. 1). The difference is that the propane oxidation in H_2O medium proceeds in several stages. At the dilution level of the reaction mixture $x_d = 60\%$ mol. (test 7), the explosion is preceded by a single peak of heat release with the maximum at $T_{out}^{max} = 541$ K, which almost coincides with the temperature T_{out}^{max} observed at the oxidation in Ar medium (test 1, Table 2), and the first maximum on curve *4* (Fig. 2) obtained at oxidation in CO_2 medium. It is obvious that the realization of a chain-thermal explosion at this temperature was prevented, first of all, by the loss of heat associated with the water evaporation. In consequence of chain-thermal explosion in H_2O medium ($x_d = 60\%$ mol.) at $T_{out}^{max} = 569$ K ($T_{out}^{max} > T_{ev}$), the maximum temperature increment $\Delta T^{max} = 778$ K and the reaction mixture temperature $T_{in}^{max} = 1345$ K were higher than those in Ar medium (test 1), despite the smaller amount of $[O_2]_0$ in test 7 comparing to test 1, as well as the greater heat capacity of $C_3H_8/O_2/H_2O$ mixture comparing to C_3H_8/O_2/Ar mixture (Tables 1 and 2).

When increasing the dilution level x_d to 70% mol. (test 10), that is, increasing the amount of water in the reaction mixture, the explosion is preceded by two peaks of heat release with the maxima at $T_{out}^{max} = 543$ and 602 K (Fig. 3), however, these maxima have a smaller temperature increment ΔT, than the first maximum on curve *7*. The increase in $[H_2O]_0$ resulted also in a decrease in the maximum temperature increment ΔT^{max} to 93 K and the temperature of the reaction mixture to 674 K, realized in the course of explosion, despite a 7% increase in the amount of $[O_2]_0$ in test 10 in comparison with test 7 (Table 1). As seen on curve *10'* (Fig. 3), at the time of the explosion (at $T_{out}^{max} = 583$ K), the pressure increment ΔP was ≈ 4.3 MPa. The dependence of $P(T_{out})$ in test 7 was not registered because of the danger of destruction of the membrane strain gauge. In general, the values S characterizing the heat release, at the propane oxidation in the Ar and H_2O media (tests 1, 7, and 10) were approximately the same, despite the longer duration of oxidation in the H_2O medium, especially in test 10 (Table 2).

From the data given in Table 1, it follows that during the propane oxidation in H_2O medium, similarly as during the oxidation in Ar medium, the values of α_f and α_O are close to 100%. Only a small amount of alkanes, alkenes, alcohols, aldehydes, and acids (Table 3) are present in the oxidation products. It is noteworthy that in test 7 ($x_d = 60\%$ mol.) the yield of H_2 is by ≈ 10 times greater than that in test 10 ($x_d = 70\%$ mol.). This is probably due to the higher rate of steam reforming reaction and water gas shift reaction

$$C_yH_z + yH_2O = yCO + (y + 0.5z)H_2, \quad (29)$$

$$CO + H_2O \leftrightarrow CO_2 + H_2, \quad (30)$$

due to the greater increment in temperature ΔT^{max} in test 7 (Table 2). Note that a high yield of H_2 is also observed as a result of chain-thermal explosion of isobutane at low density of water vapor [8].

In contrast to the propene oxidation in Ar and CO_2 media (Figs. 1 and 2), its oxidation in H_2O medium (tests 8 and 11) proceeds in two stages with the maxima observed at $T_{out}^{max} = 504$ and 590 K (Fig. 4). It can be seen in Table 2 that the propene ignition temperature in Ar, CO_2 and H_2O media is almost the same, that is, does not depend on the nature of the diluent. However, in the H_2O medium (test 8), the oxidation duration t_{ox} is longer; while the maximum temperature increment ΔT^{max} is less than in Ar and CO_2 media (tests 2 and 5, respectively). This means that the consumption of heat released during the oxidation of propene, which is required for water evaporation and increase in the heat capacity and thermal conductivity of the medium as the temperature increases (Fig. 6), prevented the increase in the oxidation rate. This is also evidenced by a decrease in the value of ΔT^{max} when increasing the dilution level up to $x_d = 71\%$ mol. in test 11 compared to test 8, despite the greater amount of $[O_2]_0$ in test 11 (Tables 1 and 2). The presence of greater amount of water in test 11 led to the fact that the value of ΔT^{max} of the second peak (at $T_{out}^{max} = 590$ K) decreased from 11 to 1 K compared to test 8 (Fig. 4). From the comparison of the S values, characterizing heat release, in tests 2, 5, and 8, it follows that in the H_2O medium ($x_d = 62\%$ mol.) the S value is almost twice as large as in Ar and CO_2 media (Table 2).

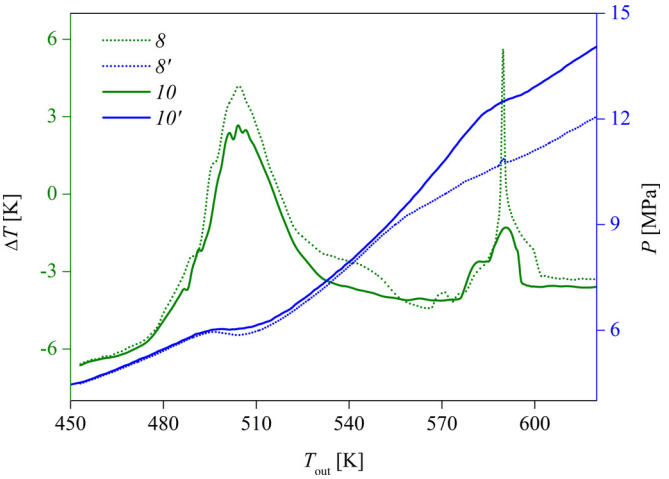

Fig. 4. Temperature dependences of difference in temperature ($\Delta T = T_{in} - T_{out}$) of reactants in the center of the reactor (T_{in}) and the external reactor wall (T_{out}), as well as pressure (P) of the reaction mixtures during propene oxidation in water vapor at the dilution level of 62 (*8, 8'*) and 71% mol. (*11, 11'*). Numbers of the curves correspond to numbers of tests in Table 1.

The results of mass spectrometric measurements (Tables 1 and 3) show that the propene oxidation in H_2O medium (test 11), in contrast to oxidation in Ar and CO_2 media (tests 2 and 5, respectively), resulted in almost complete consumption of O_2 ($\alpha_O = 98.5\%$ mol.), and the products contain only a small amount of methanol, ethanol, acetaldehyde, acetone, and acetic acid. We have previously established [11] that supercritical water suppresses the oligomerization of propene due to the manifestation of "cage effect". This means that in H_2O medium, the propene oxidation does not lead to the formation of high-boiling substances, unlike, for example, the oxidation in CO_2 medium (see Reaction (25)), that is, the processes occur mainly in the gas phase.

Oxidation of isopropanol in H_2O medium occurs in two stages (Fig. 5) similarly to oxidation in Ar and CO_2 media (Figs. 1 and 2). However, in H_2O medium, the values of self-ignition temperature T_{in}^{*} (Table 2) and the maximum temperature T_{out}^{max} of the first and second maxima on curves *9* and *12* (Fig. 5) are higher than the corresponding values obtained in oxidation of isopropanol in Ar and CO_2 media (Figs. 1 and 2). For example, the self-ignition temperature T_{in}^{*}, obtained in oxidation in H_2O medium (test 9), was by 51 and 25 K higher than that in the medium of Ar and CO_2, respectively (tests 3 and 6, Table 2). Based on the fact that the self-ignition temperature of propane and propene almost does not depend on the nature of the diluent, it can be assumed that the increase in the self-ignition temperature of isopropanol in the H_2O medium is due to its polarity (dipole moment of C_3H_7OH and H_2O molecules is 1.66 and 1.85 D, respectively) and the formation of clusters $[C_3H_7OH{\cdot}nH_2O]$.

The increase in the dilution level x_d from 61 (test 9) to 72% mol. (test 12) during the isopropanol oxidation resulted in decrease in the maximum temperature increment ΔT^{max} from 7 to 5 K, as well as shifted the second maximum of heat release from 609 to

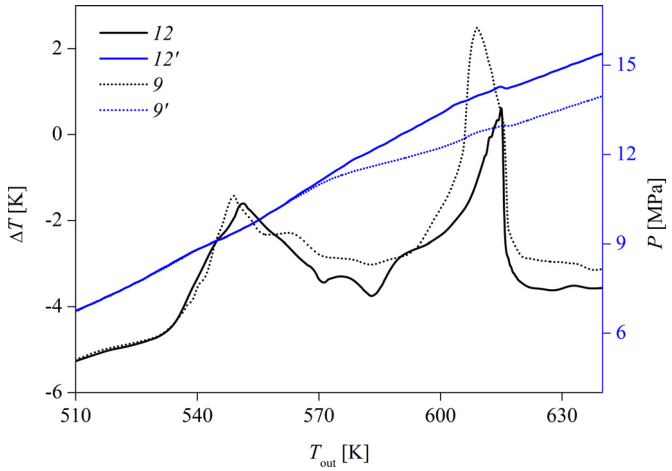

Fig. 5. Temperature dependences of difference in temperature ($\Delta T = T_{in} - T_{out}$) of reactants in the center of the reactor (T_{in}) and the external reactor wall (T_{out}), as well as pressure (P) of the reaction mixtures during isopropanol oxidation in water vapor at the dilution level of 61 (*9, 9′*) and 72% mol. (*12, 12′*). Numbers of the curves correspond to numbers of tests in Table 1.

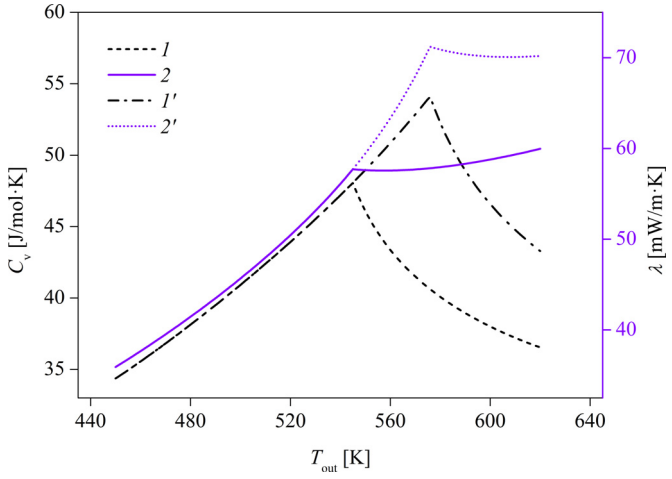

Fig. 6. Temperature dependences of heat capacity (*1, 1′*) and thermal conductivity (*2, 2′*) of saturated and superheated water vapor, corresponding to the amount of water charged into the reactor in tests 7–9 (*1, 2*) and 10–12 (*1′, 2′*) and determined by reference data [40]. Bends on the curves correspond to the complete evaporation of the water.

615 K (Table 2, Fig. 5) that reflects the increase in the heat capacity and thermal conductivity of the reaction medium with increasing temperature (Fig. 6) and heat consumption for water evaporation. Table 1 shows that, at the oxidation of isopropanol in H_2O medium, values α_f and α_O are close to 100%. Acetone, propene, acetaldehyde, acetic acid, and methanol were observed in the product (Table 3) that is consistent with the research results of isopropanol oxidation in supercritical water [21,38,39].

Based on the results obtained, we can assume that along with the chemical involvement of H_2O molecules in the elementary reactions of fuel oxidation [33,34], the processes of resonance V–V exchange between H_2O^* and O_2 molecules in the reaction [53,56]

$$H_2O^*(\nu_2 = 1595\ cm^{-1}) + O_2 \leftrightarrow H_2O + O_2^*(\nu = 1580\ cm^{-1}), \quad (31)$$

play an important role. Here ν_2 is the frequency of deformation oscillations. Since the oxidation rate by vibrationally excited O_2^* molecules is higher than by non-excited O_2 molecules [57,58], in general, this leads to increase in the specific oxidation rate of fuels (per O_2 mol.) in the H_2O medium. Note that the equilibrium fraction of $H_2O^*(\nu_2 = 1595\ cm^{-1})$ molecules at 550 K, in accordance with the Boltzmann distribution, is 1.5% of the number of molecules in the vapor phase.

According to data presented by Huestis [56], the specific rate of Reaction (31) at 300 K is equal to $5.5 \cdot 10^{-13}$ cm^3/s, while that for the translational-vibrational (T–V) exchange reaction

$$H_2O + H_2O \leftrightarrow H_2O^*(\nu_2 = 1595\ cm^{-1}) + H_2O, \quad (32)$$

is two orders of magnitude higher ($5.5 \cdot 10^{-11}$ cm^3/s). This means that the number of H_2O^* molecules, deactivated in Reaction (31), are continuously replenished in the reaction system during Reaction (32). In general, under conditions of high water density, this can contribute to the enhancement of fuels oxidation.

It follows from the results obtained that the oxidation of C_3H_8 in the H_2O medium proceeds through the mechanism of chain-thermal explosion and leads to almost complete fuel conversion and consumption of O_2, similarly as during oxidation in the Ar medium. Oxidation of C_3H_6 and C_3H_7OH in H_2O medium occurs in two stages and is characterized by almost complete consumption of O_2. In contrast to the oxidation of C_3H_8 and C_3H_6, whose self-ignition temperature is almost independent of the diluent nature, the self-ignition temperature of C_3H_7OH in the diluent medium increases in the following sequence: $Ar < CO_2 < H_2O$. The fuel oxidation dynamics in the H_2O medium is determined by the high heat capacity and thermal conductivity of water vapor, the thermal inputs for water evaporation, the involvement of H_2O molecules in elementary oxidation reactions, and vibrational energy exchange with O_2 molecules. The increase in water density contributes to the suppression of explosive oxidation modes.

4. Conclusions

In this paper, the oxidation of propane, propene, and isopropanol at high reagent density and dilution of the reaction mixture with argon, carbon dioxide, and water vapor in conditions of excess fuel is studied for the first time. Fuel excess and limited temperature range ($T \leq 640$ K) allowed identifying intermediate oxidation products, their formation mechanisms, as well as to obtain data on the self-ignition temperature of reaction mixtures. It was revealed that the oxidation of propane in Ar and H_2O media, as well as the oxidation of isopropanol in Ar and CO_2 media occurs through the chain-thermal explosion mechanism. Low degree of fuel conversion was revealed during the oxidation of propane and propene in the CO_2 medium. In the H_2O medium, oxidation of fuels occurs in several stages and is characterized by almost complete consumption of O_2. It follows from the results obtained that the chain-thermal explosion in the fuels oxidation occurs in the region of the system parameters (T, P), which essentially depend not only on the chemical structure of the fuel and the concentration of reagents, but also on the nature of the diluent.

Acknowledgments

The authors gratefully acknowledge M.Y. Sokol for assistance during the experiments. This study was supported by the Russian Foundation for Basic Research (Grant no. 18-29-06005).

References

[1] J.P.S. Queiroz, M.D. Bermejo, F. Mato, M.J. Cocero, Supercritical water oxidation with hydrothermal flame as internal heat source: Efficient and clean energy production from waste, J. Supercrit. Fluids 96 (2015) 103–113.
[2] Q. Yan, Y. Hou, J. Luo, H. Miao, H. Zhang, The exergy release mechanism and exergy analysis for coal oxidation in supercritical water atmosphere and a power generation system based on the new technology, Energy Conv. Manag. 129 (2016) 122–130.

[3] Z. Chen, X. Zhang, S. Li, L. Gao, Novel power generation models integrated supercritical water gasification of coal and parallel partial chemical recovery, Energy 134 (2017) 933–942.
[4] K.J. Borgert, E.S. Rubin, Oxy-combustion carbon capture for pulverized coal in the integrated environmental control model, Energy Proc. 114 (2017) 522–529.
[5] S. Chen, Fundamentals of oxy-fuel combustion, in: Z. Chuguang, L. Zhaohui (Eds.), Oxy-Fuel Combustion: Theory and Practice, Elsevier, 2018, pp. 13–30.
[6] A.A. Vostrikov, O.N. Fedyaeva, A.V. Shishkin, D.S. Tretyakov, M.Y. Sokol, Features of low temperature oxidation of hydrogen in the medium of nitrogen, carbon dioxide, and water vapor at elevated pressures, Int. J. Hydrog. Energy 43 (2018) 10469–10480.
[7] A.A. Vostrikov, O.N. Fedyaeva, A.V. Shishkin, M.Y. Sokol, F.I. Kolobov, V.I. Kolobov, Partial and complete methane oxidation in supercritical water, J. Eng. Thermophys. 25 (4) (2016) 474–484.
[8] A.A. Vostrikov, O.N. Fedyaeva, A.V. Shishkin, D.O. Artamonov, M.Y. Sokol, Features of low-temperature oxidation of isobutane in water vapor and carbon dioxide with increased density of reagents, J. Eng. Thermophys. 26 (4) (2017) 466–475.
[9] Y.M. Alshammari, K. Hellgardt, Sub and supercritical water reforming of n-hexadecane in a tubular flow reactor, J. Supercrit. Fluids 107 (2016) 723–732.
[10] O.N. Fedyaeva, V.R. Antipenko, A.A. Vostrikov, Peculiarities of composition of hydrocarbon and heteroatomic substances obtained during conversion of Kashpir oil shale in supercritical water, Russ. J. Phys. Chem. B 11 (2017) 1246–1254.
[11] O.N. Fedyaeva, A.A. Vostrikov, V.R. Antipenko, A.V. Shishkin, V.I. Kolobov, M.Y. Sokol, Role of supercritical water and pyrite in transformations of propylene, Russ. J. Phys. Chem. B 11 (2017) 1117–1128.
[12] S.S. Merchant, C.F. Goldsmith, A.G. Vandeputte, M.P. Burke, S.J. Klippenstein, W.H. Green, Understanding low-temperature first-stage ignition delay: propane, Combust. Flame 162 (2015) 3658–3673.
[13] J.C. Prince, F.A. Williams, Short chemical-kinetics mechanisms for low-temperature ignition of propane and ethane, Combust. Flame 159 (2012) 2336–2344.
[14] F. Norman, F. Van den Schoor, F. Verplaetsen, Auto-ignition and upper limit of rich propane-air mixtures at elevated pressures, J. Hazard. Mater. A 137 (2006) 666–671.
[15] R.D. Wilk, N.P. Cernansky, R.S. Conen, An experimental study of propene oxidation at low and intermediate temperature, Combust. Sci. Technol. 52 (1987) 39–58.
[16] M.S. Stark, D.J. Waddington, Oxidation of propene in the gas phase, Int. J. Chem. Kinet. 27 (1995) 123–151.
[17] S.G. Davis, C.K. Law, H. Wang, Propene pyrolysis and oxidation kinetics in a flow reactor and laminar flames, Combust. Flame 119 (1999) 375–399.
[18] S.M. Burke, W. Metcalfe, O. Herbinet, F. Battin-Leclerc, F.M. Haas, J. Santner, F.L. Dryer, H.J. Curran, An experimental and modeling study of propene oxidation. Part 1: Speciation measurements in jet-stirred and flow reactors, Combust. Flame 161 (2014) 2765–2784.
[19] S.M. Burke, U. Burke, R. Mc Donagh, O. Mathieu, I. Osobio, C. Keesee, A. Morones, E.L. Petersen, W. Wang, T.A. DeVerter, M.A. Oehlschlaeger, B. Rodes, R.H. Hanson, D.F. Davidson, B.W. Weber, C.-J. Sung, J. Santner, Y. Ju, H.J. Curran, An experimental and modeling study of propene oxidation. Part 2: Ignition delay time and flame speed measurements, Combust. Flame 162 (2015) 296–314.
[20] S.M. Sarathy, P. Oβwald, N. Hansen, K. Korse-Höinghaus, Alcohol combustion chemistry, Prog. Energy Combust. Sci. 44 (2014) 40–102.
[21] J. Abelleira, J. Sanchez-Oneto, J.R. Portela, E.J. Martinez de la Ossa, Kinetics of supercritical water oxidation of isopropanol as an auxiliary fuel and co-fuel, Fuel 111 (2013) 574–583.
[22] P. Cabeza, J.P.S. Queiroz, M. Criado, C. Jimenez, M.D. Bermejo, M.J. Cocero, Supercritical water oxidation for energy production by hydrothermal flame as internal heat source. Experimental results and energetic study, Energy 90 (2015) 1584–1594.
[23] B. Al Duri, F. Alsoqyiani, I. Kings, Supercritical water oxidation (SCWO) for the removal of N-containing heterocyclic hydrocarbon wastes. Part I: Process enhancement by addition of isopropyl alcohol, J. Supercrit. Fluids 116 (2016) 155–163.
[24] Y. Li, L. Wei, Z. Tian, B. Yang, J. Wang, T. Zhang, F. Qi, A comprehensive experimental study of low-pressure premixed C3-oxygenated hydrocarbon flames with tunable synchrotron photoionization, Combust. Flame 152 (2008) 336–359.
[25] T. Kasper, P. Oβwald, U. Struckmeier, K. Kohse-Höinghaus, C.A. Taatjes, J. Wang, T.A. Cool, M.E. Law, A. Morel, P.R. Westmoreland, Combustion chemistry of the propanol isomers – investigated by electron ionization and VUV-photoionization molecular-beam mass-spectrometry, Combust. Flame 156 (2009) 1181–1201.
[26] A. Franssoldati, A. Cuoci, T. Faravelli, U. Nuemann, E. Ranzi, R. Seiser, K. Seshardri, An experimental and kinetic study of propanol and iso-propanol combustion, Combust. Flame 157 (2010) 2–16.
[27] X. Man, C. Tang, J. Zhang, Y. Zhang, L. Pan, Z. Huang, C.K. Law, An experimental and kinetic modeling study of n-propanol and i-propanol ignition at high temperatures, Combust. Flame 161 (2014) 644–656.
[28] S. Jouzdani, A. Zhou, B. Akih-Kumgeh, Propanol isomers: Investigation of ignition and pyrolysis time scales, Combust. Flame 176 (2017) 229–244.
[29] A. Abdelkhalik, E. Askar, D. Markus, E. Brandes, I. El-Sayed, M. Hassan, M. Nour, T. Stolz, Explosion regions of propane, isopropanol, acetone, and methyl acetate/inert gas/air mixtures, J. Loss Prev. Proc. Ind. 43 (2016) 669–675.
[30] W. Ebina, C. Liao, H. Naito, A. Yoshida, Effect of water mist on minimum ignition energy of propane/air mixture, Proc. Combust. Inst. 36 (2017) 3271–3278.
[31] W. Zhang, X. Gou, Z. Chen, Effect of water vapor dilution on the minimum ignition energy of methane, n-butane and n-decane at normal and reduced pressures, Fuel 187 (2017) 111–116.
[32] T. Le Cong, E. Bedjanian, P. Dagaut, Oxidation of ethylene and propene in the presence of CO_2 and H_2O: Experimental and detailed kinetic modeling study, Combust. Sci. Tech. 182 (4–6) (2010) 333–349.
[33] M. Lubrano Lavadera, P. Sabia, M. De Joannon, A. Cavaliere, R. Ragguci, Propane oxidation in a jet stirred flow reactor. The effect of H_2O as diluent species, Exp. Thermal Fluid Sci. 95 (2018) 35–43.
[34] R.H. Holgate, J.W. Tester, Oxidation of hydrogen and carbon monoxide in sub- and supercritical water: reaction kinetics, pathways, and water-density effects. 2. Elementary reaction modelling, J. Phys. Chem. 98 (1994) 810–822.
[35] P. Sabia, M. Lubrano Lavadera, P. Guidicianni, G. Sorrentino, R. Ragguci, M. de Joannon, CO_2 and H_2O effect on propane auto-ignition delay times under mild combustion operative conditions, Combust. Flame 162 (2015) 533–543.
[36] F. Liu, H. Guo, G.J. Smallwood, The chemical effect of CO_2 replacement N_2 in air on burning velocity of CH_4 and H_2 premixed flame, Combust. Flame 133 (2003) 495–497.
[37] A.E. Masunov, E.E. Wait, A.A. Atlanov, S.S. Vasu, Quantum chemical study of supercritical carbon dioxide effects on combustion kinetics, J. Phys. Chem. A 121 (2017) 3728–3735.
[38] T.B. Hunter, S.F. Rice, R.G. Hanush, Raman spectroscopic measurement of oxidation in supercritical water. 2. Conversion of isopropyl alcohol to acetone, Ind. Eng. Chem. Res. 35 (1996) 3984–3990.
[39] M. Krajnc, J. Levec, Catalytic oxidation of toxic organics in supercritical water, Appl. Catal. B Environ. 3 (1994) 101–107.
[40] E.W. Lemmon, M.O. McLinden, D.G. Freid, Thermophysical properties of fluid systems, in: P.J. Linstrom, W.G. Mallard (Eds.), NIST Chemistry WebBook, NIST Standard Reference Database No 69, National Institute of Standards and Technology, Gaithersburg MD, 2017, p. 20899 http://webbook.nist.gov/chemistry/fluid/.
[41] A.M. Bogomolnyi (Ed.), Physical and chemical properties of organic substances: handbook, Khimiya, Moscow, 2008 [In Russian].
[42] O.N. Fedyaeva, A.A. Vostrikov, A.V. Shishkin, M.Y. Sokol, N.I. Fedorova, V.A. Kashirtsev, Hydrothermolysis of brown coal in cyclic pressurization-depressurization mode, J. Supercrit. Fluids 62 (2012) 155–164.
[43] A.Y. Guva, Brief thermophysical handbook, Sibvuzizdat, Novosibirsk, 2002 [In Russian].
[44] L.V. Gurvich, G.V. Karachentzev, V.N. Kondratiev, Yu.A. Lebedev, V.A. Medvedev, V.K. Potapov, Yu.S. Hodeev, Break energies of chemical bonds. Ionization potentials and electron Affinity, Nauka, Moscow, 1974 [In Russian].
[45] F. Xin, M. Xu, X. Huai, X. Li, Study on isopropanol-acetone-hydrogen chemical heat pump: Liquid phase dehydrogenation of isopropanol using a reactive distillation column, Appl. Thermal Eng. 58 (2013) 369–373.
[46] N.N. Semenov, Some problems of chemical kinetics and reactivity, Izd. AN SSSR, Moscow, 1958 [In Russian].
[47] D.A. Frank-Kamenetskii, Diffusion and heat exchange in chemical kinetics, Nauka, Moscow, 1987 [In Russian].
[48] H.B. Biu, R.S. Zhu, M.C. Lin, Thermal decomposition of iso-propanol: First-principles prediction of total and product-branching rate constant, J. Chem. Phys. 117 (2002) 11188–11195.
[49] C. Zhang, S. Li, L. Wang, T. Wu, S. Peng, Studies on the decomposing carbon dioxide into carbon with oxygen-deficient magnetite. II. The effects of properties of magnetite on activity of decomposition CO_2 and mechanism of the reaction, Mater. Chem. Phys. 62 (2000) 52–61.
[50] A.A. Vostrikov, O.N. Fedyaeva, A.V. Shishkin, M.Y. Sokol, A.V. Zaikovskii, Synthesis of Fe_xO_y nanoparticles during iron oxidation by supercritical water, Tech. Phys. Lett. 38 (2012) 955–958.
[51] L. Gharnati, N.E. Musko, A.D. Jensen, G.M. Kontogeorgis, J.-D. Grunwaldt, Fluid phase equilibria during propylene carbonate synthesis from propylene oxide in carbon dioxide medium, J. Supercrit. Fluids 82 (2013) 106–115.
[52] D.-H. Lan, F.-M. Yang, S.-L. Luo, C.-T. Au, S.-F. Yin, Water-tolerant graphene oxide as a high-efficiency catalyst for the propylene carbonate from propylene oxide and carbon dioxide, Carbon 73 (2014) 351–360.
[53] V.N. Kondratiev, E.E. Nikitin, Kinetic and mechanism of gas-phase reactions, Nauka, Moscow, 1974 [In Russian].
[54] Computational chemistry comparison and benchmark data base, release 18, in: R.D. Johnson III (Ed.), Standard Reference Database 101, National Institute of Standards and Technology, 2018 http://cccbdb.nist.gov/.
[55] A.A. Vostrikov, S.G. Mironov, The role of van der Waals molecules in vibrational relaxation kinetics, Chem. Phys. Lett. 101 (6) (1983) 583–587.
[56] D.L. Huestis, Vibrational energy transfer and relaxation in O_2 and H_2O, J. Phys. Chem. A 110 (2006) 6638–6642.
[57] A.M. Starik, N.S. Titova, V.I. Loukhovitski, Kinetics of low-temperature initiation of $H_2/O_2/H_2O$ mixture combustion upon the excitation of molecular vibrations in H_2O molecules by laser radiation, Tech. Phys. 49 (2004) 76–82.
[58] N.A. Popov, The effect of nonequilibrium excitation on the ignition of hydrogen-oxygen mixtures, High Temp. 45 (2) (2007) 261–279.